Available online at www.sciencedirect.com

SCIENCE DIRECT®

Journal of Nuclear Materials 334 (2004) 200–206

journal of nuclear materials

www.elsevier.com/locate/jnucmat

Analysis on volume fraction and crystal orientation relationship of monoclinic and tetragonal oxide grown on Zr–2.5Nb alloy

Jianlong Lin *, Hualong Li, Cheol Nam, Jerzy A. Szpunar

Department of Metallurgical Engineering, McGill University, Montreal, Canada H3A 2B2

Received 11 February 2004; accepted 9 June 2004

Abstract

Texture and phase volume fraction of the oxide grown on Zr–2.5Nb, in static autoclaves, at 623 K, with lithiated heavy water were investigated. It is found that both monoclinic and tetragonal zirconia are highly textured with $\{100\}\langle 100\rangle$ preferred crystal orientation for the tetragonal phase, and $(10\bar{3})[0\bar{1}0]$ and $(10\bar{4})[401]$ texture for the monoclinic phase. No change in the texture for both phases was observed with the increase of thickness of the oxide layer. The crystal orientation relationship of both the monoclinic and tetragonal phases was found to be $(10\bar{3})_m \| (100)_t$ or $(10\bar{3})_m \| (101)_t$ and $[100]_t \| [010]_m$. The integrated intensity over pole figures was used to calculate the volume fraction of the tetragonal phase in the oxide layer. The volume fraction of the tetragonal phase in the dense oxide layer near the metal–oxide interface was found to be about 8% and gradually decreases with an increase of the oxide thickness.

PACS: 28.52.Fa

1. Introduction

Along with circumferential expansion, creep sag, and irradiation growth, hydrogen ingress and formation of zirconium hydride are major factors that affect the lifetime of the Zr–2.5Nb pressure tubes [1]. In the final stage of manufacturing Zr–2.5Nb pressure tubes, the tube is annealed in steam environment at 675 K for 24 h [2]. The purpose of this procedure is two-fold: to release the stress in the pressure tube caused by extrusion during its manufacturing process and to form a thin zirconium oxide layer on the surface of the pressure tube. Like any other materials, the properties of zirconium oxide are dependent on its microstructure and are affected by the existence of strong crystallographic texture. Zirconium oxidation is controlled by an inward diffusion of oxygen, and the knowledge of texture and structure of the oxide layer is of technological importance because this layer controls the oxidation process and hydrogen ingress into the tube. The oxide layer grown on Zr–2.5Nb is predominantly monoclinic (m) zirconia, however Raman spectroscopy studies [3] and TEM [4,5] demonstrated that small amount of tetragonal zirconia (t) is present in the oxide layer. Khatamian and Lalonda [6] referred the minor phase as nearly cubic-tetragonal (nct) phase to differentiate it from the tetragonal phase existing above 1400 K with the $c/a = 1.451$ [7].

---

* Corresponding author.
E-mail address: jianlong.lin@mail.mcgill.ca (J. Lin).

0022-3115/$ - see front matter © 2004 Elsevier B.V. All rights reserved.
doi:10.1016/j.jnucmat.2004.06.003

It was demonstrated that there is a higher percentage of tetragonal phase in the inner oxide layer near the oxide–metal interface than at the outer oxide layer. The compressive stress described by Pilling–Bedworth, for a ratio 1.56 of Zr/ZrO_2, is considered as the main factor that stabilizes the tetragonal phase in the inner layer. The amount of tetragonal phase can be as high as 40% of the volume in the layer near the oxide–metal interface [8]. The acceleration of the oxidation rate in lithiated water (70 ppm Li) seems to be linked to a gradual disappearance of the tetragonal zirconium oxide phase [9]. In general, it is accepted that the phase transition from tetragonal to monoclinic is associated with the oxidation acceleration. When the oxide grows, the tetragonal phase is transformed to the monoclinic phase, which causes the formation of pores and cracks in the oxide layer. Because those pores and cracks serve as fast paths for oxygen diffusion through the oxide layer, the oxide layer cannot serve as a barrier against oxygen diffusion.

Properties of monoclinic zirconia were studied extensively, however much less attention was paid to tetragonal zirconia, whose presence is believed to be associated with acceleration of oxidation kinetics in Zr–2.5Nb. Detailed information on tetragonal zirconia structure is important to understand the oxide growth mechanism. In this paper the transformation of texture and volume fraction of the tetragonal phase in the process of oxide growth will be analyzed.

2. Experimental procedure

2.1. Samples preparation and texture measurement

Zr–2.5Nb samples of dimension $30 \times 15 \times 1$ mm were machined from a pressure tube. The tube was extruded at 1093–1123 K, cold worked by 20–30% and then stress relieved in steam for 24 h at 673 K. The specimens were cut so that the direction normal to their surface coincides with the radial direction of the tube. All samples were grounded using SiC paper down to 1200 grit and pickled prior to the autoclave tests with an acid mixture of 10% HF + 15% HNO_3 + 30% H_2SO_4 + 45% H_2O.

Specimens were oxidized in static autoclaves at 623 K with lithiated heavy water, $pH_{25\,°C} \cong 10.4$, for different times. The Schulz reflection method [10] was used to measure pole figures. The measurements were performed on a Siemens D-500 texture goniometer using copper X-ray tube. The $(11\bar{1})_m$, $(111)_t$, $(111)_m$ and $(002)_m$ pole figures were measured for all oxide layers, where subscripts t and m indicate tetragonal and monoclinic phases, respectively. To correct the experimental data, texture free samples of ZrO_2 powder were measured under the same conditions as the investigated textured specimens.

2.2. Calculation of volume fraction of tetragonal phase

The determination of the volume fraction of tetragonal oxide phase formed in different media has been attempted by many authors [5,11], mainly because the existence of this phase is related to properties of the barrier against oxygen diffusion near the metal/oxide interface. Conventional X-ray diffraction techniques can be used to determine the relative amounts of various phases if the oxide layer is made into powder. This method is however destructive because the oxide has to be removed from the substrate and ground into powder. The removal of the oxide from the metal will result in a relaxation of stresses [12], leading to a change of relative amounts of different phases [8,13,14] because the tetragonal phase is stabilized by compressive stresses. Thus, the measurement of phase composition should be performed without removing the oxide film from the metal substrate. Simple XRD scans made on these samples did not allow quantitative determination of the amount of tetragonal and monoclinic phases, due to the existence of texture in oxide films. Therefore, large errors can be introduced into the determination of phase composition if the texture effect is not taken into account of the calculation.

The technique reported by Glavicic et al. [15] allows the quantitative determination of relative volume fractions of phases in multiphase textured materials, by averaging the intensity over measured pole figures. The technique is based on the polymorph method developed by Garvie and Nicholson [16] to analyze a mixture of texture free powders of monoclinic and tetragonal zirconia. The integrated intensities $I_t(hkl)$ of the $(11\bar{1})_m$, $(111)_m$ monoclinic and $(111)_t$ tetragonal pole figures were used to determine the tetragonal zirconia volume fraction with respect to the total volume of zirconia using the equation:

$$X_t = \frac{V_t}{V_m + V_t} = \frac{I_t(111)_t}{C[I_t(11\bar{1})_m + I_t(111)_m] + I_t(111)_t} \tag{1}$$

with

$$C = R(111)_t/[R(11\bar{1})_m + R(111)_m].$$

The theoretical intensities $R(hkl)_t$ of the considered diffraction lines and the related coefficient C, can be calculated for different radiations used. For Cu Kα, the coefficient C is 1.381 [17].

3. Results and discussion

3.1. Texture of monoclinic and tetragonal zirconia phase

The oxidation time of the samples for texture studies was varied from 3 days to 227 days. The oxide thickness increases from 0.76 to 4.58 μm with increasing oxidation time. The results presented in Fig. 1 show that both the monoclinic phase and the tetragonal phase are strongly textured.

Orientation distribution function (ODF) is a mathematical representation of the measured texture which describes the frequencies of various spatial orientation of the crystal reference frame within the sample reference frame. The ODF of tetragonal zirconia was calculated from the pole figure $(111)_t$ using TexTools software [18]. The tetragonal phase lattice parameters $a = 5.05$ nm, $c = 5.14$ nm and ratio $c/a = 1.018$, were determined from RHEED results of zirconia layer grown on Zr–2.5Nb alloy [6], are selected for ODF calculation. As an example, Fig. 2 shows calculated ODFs for monoclinic and tetragonal zirconia grown on Zr–2.5Nb sample with the oxidation time of 47 days (corresponding to oxide thickness is 1.7 μm). The maximum intensity of 21.8 is at Euler angles $\varphi_1 = 0$, $\psi = 0$, $\varphi_2 = 0$ and the ideal crystal orientation of tetragonal zirconia can be described as $\{100\}\langle 100\rangle$, which means that the $\{100\}$ plane is parallel to the surface of the sample and the $\langle 100\rangle$ direction is parallel to the axial direction of the pressure tube. The accuracy of calculated ODF intensity

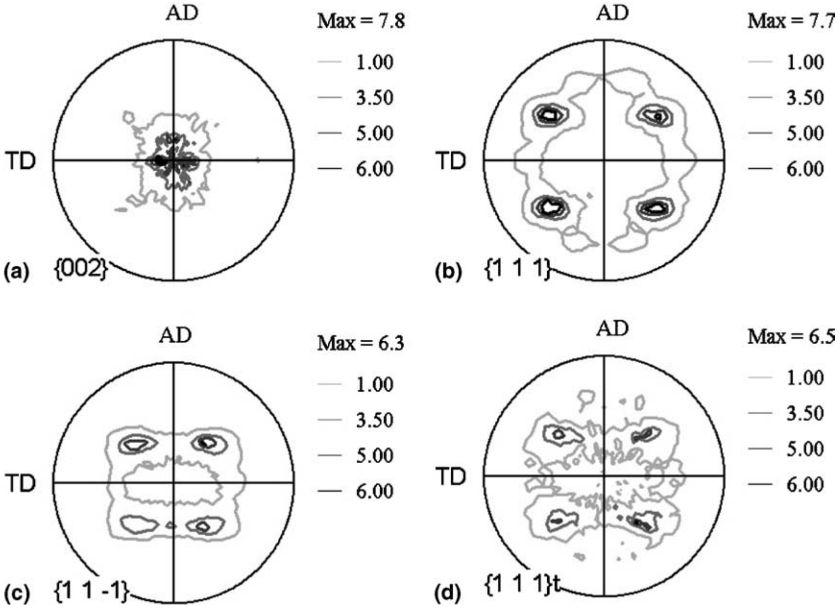

Fig. 1. Measured pole figures for the oxide layer (a) (002), (b) (111), and (c) $(11\bar{1})$ monoclinic; (d) $(111)_t$ tetragonal. Oxide layer thickness is 1.7 μm.

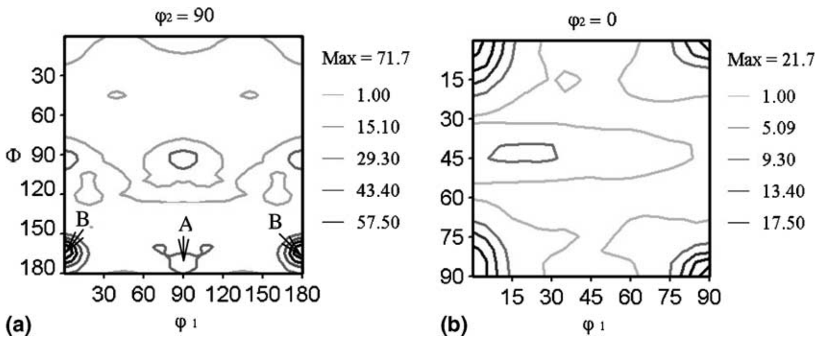

Fig. 2. Calculated ODF (a) section $\varphi_2 = 90°$ monoclinic zirconia phase (b) section $\varphi_2 = 0°$ tetragonal zirconia phase, for oxide having a thickness of 1.7 μm grown on Zr–2.5Nb specimen.

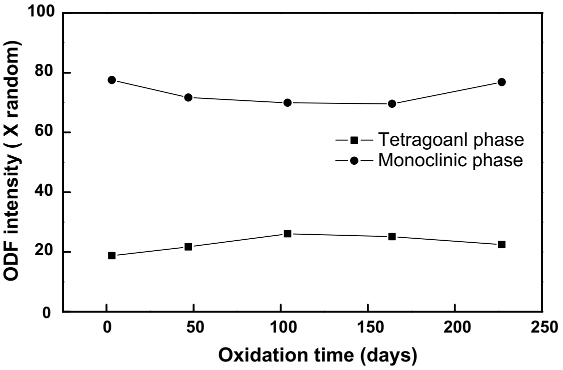

Fig. 3. Maximum ODF intensity of monoclinic and tetragonal phases vs. exposure time of Zr–2.5Nb specimen.

is dependent on statistical reliability of the measurements and the number of pole figures used as the input data for the calculation. The higher the number of pole figures, the more accurate the ODF calculation result. In our studies, only one reflection peak (1 1 1) of tetragonal phase in zirconium oxide layer was clearly identified by X-ray diffraction method and was used for pole figure measurement. Considering that the ODF is calculated from only one pole figure, there might be some error in the intensity of ODF and associated volume fraction of texture component. However, the calculated preferred crystal orientation based on this method is reliable.

The ODF of monoclinic zirconia was calculated from $(11\bar{1})$, (1 1 1) and (0 0 2) pole figures. The calculated ODF for the sample with oxide thickness $t = 1.7$ μm is shown in Fig. 2. This result clearly demonstrates that there are two preferred crystal orientations, $(10\bar{3})[0\bar{1}0]$ and $(10\bar{4})[401]$ for monoclinic phase. It is clearly shown in Fig. 2 that the intensity of ideal orientation of $(10\bar{3})[0\bar{1}0]$ (marked by B) is much higher than that of $(10\bar{4})[401]$ (marked by A) and therefore the orientation B is considered as the major texture component in monoclinic phase. The ODF calculated for all samples shows that there is no change in texture type with the oxidation time increasing, or with the increase of the thickness of the zirconium oxide layer.

Comparing the ODF intensity of monoclinic phase to the tetragonal phase among all the samples as shown in Fig. 3, one can see that the trend of ODF intensity of monoclinic phase change is inversely proportional to the trend of ODF intensity of tetragonal phase. It has been demonstrated that the tetragonal phase transforms to the monoclinic phase during the oxidation process [8] because of the reduction of the compression stress in the oxide film. When the monoclinic to tetragonal phase transformation occurs, the crystal orientation relationship is of great interest because it may help to understand the mechanism of transformation. This orientation relationship can be derived from statistical analysis of the texture information of both phases. Inverse pole figure has been adopted to illustrate statistical orientation relationship. Fig. 4 shows the ND (normal direction, $\alpha = 0$, $\beta = 0$) inverse pole figure of both monoclinic phase and tetragonal phase. It indicates that for the monoclinic phase, the maximum intensity corresponds to $[10\bar{6}]$ direction, which is perpendicular to the $(10\bar{3})$ plane in monoclinic ZrO_2 system. Because structure of tetragonal zirconia can be treated as near cubic system with its $c/a = 1.018$. $[hkl]$ direction in this case can be treated as being the normal direction of (hkl) plane. From the ND inverse pole figures shown in Fig. 4, it is evident that, during the phase transformation from tetragonal to monoclinic oxide, the crystal orientation relationship of the two different structures along the normal direction of the pressure tube is: $(10\bar{3})_m \| (100)_t$ or $(10\bar{3})_m \| (101)_t$, where m stands for monoclinic phase and t stands for tetragonal phase. This conclusion is supported by the ZrO_2 film texture formation model proposed by Li et al. [19]. According to this model, the oxide crystallographic orientation which can reduce the planar compressive stress in the oxide film is favorable during the oxide growth. Thus, in the tetragonal system, the oxide orientations with {1 0 0} parallel to the sample surface will be the most favorable during oxide growth. For monoclinic oxide, the $(10\bar{3})$ orientations are the most favorable in reducing the stress parallel to the surface of the oxide film and this has been verified experimentally [19]. Therefore, it can be concluded that the orientation relationship between the

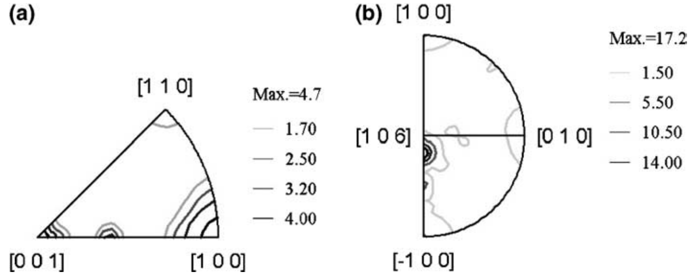

Fig. 4. Inverse pole figures for (a) tetragonal and (b) monoclinic phase for the normal direction (ND, $\alpha = 0$, $\beta = 0$).

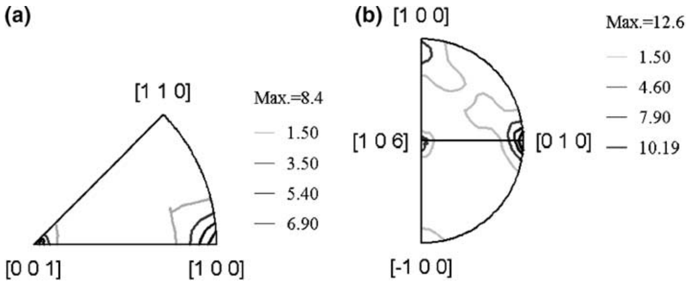

Fig. 5. Inverse pole figures for (a) tetragonal and (b) monoclinic phase for the axial direction (AD, $\alpha = 90$, $\beta = 0$).

tetragonal and monoclinic oxide during the phase transformation is governed by compressive stress in the oxide film. In order to keep the low compressive stress, the oxide orientations simply change from the most favorable tetragonal orientations to the most favorable monoclinic orientations as the phase transformation occurs.

The above discussion explains the orientation relationship between tetragonal and monoclinic oxides along the direction normal to the pressure tube. Fig. 5 illustrates the inverse pole figures for the monoclinic phase and the tetragonal phase for the axial direction of the pressure tube. The maximum intensity for the monoclinic phase is the [0 1 0] direction, while the maximum of intensity for the tetragonal phase corresponds to the [1 0 0] direction. It is clear that the $[010]_m$ direction of monoclinic phase is parallel to the $[100]_t$ direction of tetragonal phase.

The oxidation condition has little effect on the formation of the texture of the oxide. In our research work, the texture of zirconia is same as the results obtained by Glavicic et al. [15] when the oxide was grown on Zr–2.5Nb samples with the same substrate texture, but at different oxidation temperature and in different oxidation media. Our experimental results of oxidation in air environment also confirm that the oxidation condition has no effect on the texture of the oxide. These results will be discussed in another paper. However, the texture of zirconia grown on Zr–2.5Nb is strongly affected by the texture of the substrates. Petigny et al. [20] demonstrated that $(10\bar{4})$ and $(10\bar{3})$ fiber textures for monoclinic oxide developed on the recrystallized Zr–2.5Nb sheet, while in our case $(10\bar{3})[0\bar{1}0]$ and $(10\bar{4})[401]$ texture for monoclinic oxide was found in the oxide layer grown on Zr–2.5Nb pressure tube substrates.

3.2. Quantitative phase analysis

The calculation of volume fraction of tetragonal phase was based on the method discussed earlier. Fig. 6 presents the changes of the tetragonal volume fraction, the weight-gain of the samples of Zr–2.5Nb as a function of exposure time and a decrease in the percentage of the volume fraction of the tetragonal phase with increasing time. The results are in agreement with those obtained by other authors [8,11,15,20–22]. For the sample with an exposure time 3 days, the thickness of the oxide layer was ~760 nm and the volume fraction of tetragonal phase is around 8%. According to the RHEED results [6], the thickness of the dense layer near the interface is between 200 and 800 nm. If we assume that there is no phase transformation occurring for the sample with the thickness of oxide around 760 nm, this oxide layer can be regarded as inner dense oxide layer. Our experimental result suggests that the volume fraction of tetragonal phase in the dense layer near the oxide–metal interface is close to or higher than 8%.

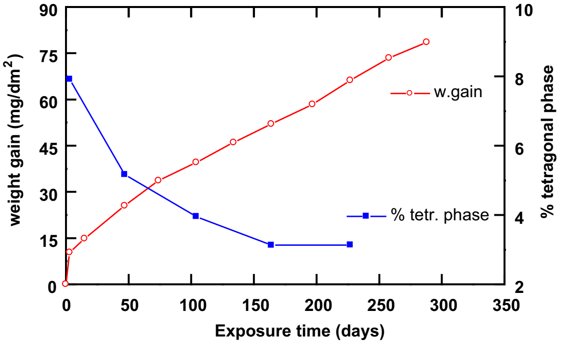

Fig. 6. Oxidation kinetics and computed volume fraction of the tetragonal phase vs. exposure time of Zr–2.5Nb specimen.

The penetration depth of X-ray is dependent on the angle of incidence of X-ray beam on the specimen surface and the mass absorption coefficient of investigated material. In symmetrical reflection geometry, the incident angle for (1 1 1) peak of tetragonal phase is 15.14°. The X-ray penetration depth t, is defined here as the distance from the sample surface at which the diffraction intensity from the inner layer decreases to the one-thousandth of that from the surface layer. This penetration depth can be calculated from the following formula [23]:

$$t = 3.45 \sin\theta/\mu, \tag{2}$$

where μ is linear absorption coefficient of zirconia and its value is 581.84 cm^{-1}.

The X-ray penetration depth calculated using formula (2) is around 15 μm and this value is higher than the oxide thickness of all samples (the maximum oxide thickness is less than 5 μm in our case). Therefore, it is reasonable to assume that the integrated intensity over the pole figure reflects the diffracted intensity from the tetragonal phase from the entire oxide layer. It is known that zirconia grown on Zr–2.5Nb is a multilayer structure and it consists of a dense inner oxide layer near the metal–oxide interface and a porous and fractured outer layer. The tetragonal phase content is higher in the dense layer near the metal–oxide interface. Therefore, the increase of the thickness of oxide film is associated with the transformation from the tetragonal to the monoclinic phase which decreases the percentage of tetragonal phase in the entire oxide. At this point, our results cannot indicate at what oxide thickness the tetragonal to monoclinic phase transformation takes place and what the mechanics of the transformation is. However, tetragonal to monoclinic phase transformation has been investigated in zirconia ceramics and the mechanics of the phase transformation has been proposed [24]. No matter at what oxide thickness the phase transformation takes place, our results indicate that the volume fraction of tetragonal zirconia is around 8% in the dense layer near the metal–oxide interface and it declines with the increase of the oxide thickness. The value we found is lower than the 40% reported by Godlewski et al. [8] and the 30–35% reported by Petigny et al. [20] when the texture of the oxide was not taken into account in these investigations, but is similar to the value obtained by latter authors when their results were corrected for oxide texture. The same calculation method was also applied to Zircaloy-4, which has different substrate texture from Zr–2.5Nb. The volume fraction of tetragonal phase in the oxide layer grown on Zircaloy-4 is higher than that in the oxide layer grown on Zr–2.5Nb [25]. The method that we used to calculate the phase composition is reliable because the effect of strong texture in the oxide layer was taken into consideration.

4. Conclusions

The texture and the phase composition of zirconium oxide layer grown on Zr–2.5Nb alloy have been investigated. The results show that tetragonal and monoclinic zirconia in the oxide are strongly textured with the ideal crystal orientation of tetragonal phase being $\{001\}\langle 100\rangle$, while $(10\bar{3})[0\bar{1}0]$ and $(10\bar{4})[401]$ orientation are identified in the monoclinic phase. Texture of the monoclinic phase oxide is about 4 times stronger than that of the tetragonal phase. No change in texture of both phases was observed with the increase of oxidation time. The crystal orientation relationship between monoclinic phase and tetragonal phase can be described as $(10\bar{3})_\mathrm{m}\|(100)_\mathrm{t}$ or $(10\bar{3})_\mathrm{m}\|(101)_\mathrm{t}$ and $[100]_\mathrm{t}\|[010]_\mathrm{m}$. The volume fraction of both monoclinic and tetragonal phases was calculated using integrated intensity over the pole figures to eliminate the effect of texture in the oxide on phase composition calculation. In addition, the results obtained indicate that the volume fraction of tetragonal zirconia is around 8% in the dense layer near the metal–oxide interface and it decreases with the increase of the oxide thickness.

References

[1] E.F. Ibrahim, B.A. Cheadle, Can. Metall. Quart. 24 (3) (1985) 273.

[2] V.F. Urbanci, B.D. Warr, A. Manolescu, C.K. Chow, M.W. Shanahan, in: Proceedings of 8th International Symposium on zirconium in the Nuclear Industry, ASTM-STP, 1989, p. 20.

[3] Y.P. Lin, O.T. Woo, D.J. Lockwood, Mater. Res. Soc. Symp. Proc. 343 (1994) 487.

[4] H. Beie, A. Mitwalsky, F. Garzarolli, H. Ruhmann, H. Sell, in: Proceedings of 10th International Symposium on Zirconium in the Nuclear Industry, ASTM-STP 1245, 1994, p. 615.

[5] H. Anada, K. Takeda, 11th Int. Symp. on Zirconium in the Nuclear Industry, ASTM-STP 1295 (1996) 35.

[6] D. Khatamian, S.D. Lalonda, J. Nucl. Mater. 245 (1997) 10.

[7] A.S. Foster, V.B. Sulimov, F. Lopez Gejo, A.L. Shluger, R.M. Nieminen, Phys. Rev. B 64 (2001) 224108.

[8] J. Godlewski, J.P. Gross, M. Lambertin, M. Wadier, J.F. Weidinger, in: Proceedings of 9th International Symposium on Zirconium in the Nuclear Industry, ASTM-STP 1132, 1991, p. 416.

[9] D. Pecheur, J. Godlewski, J. Peybernes, L. Fayette, M. Noe, A. Frichet, O. Kerrec, in: Proceedings of 12th International Symposium on Zirconium in the Nuclear Industry, ASTM STP 1354, 1998, p. 793.

[10] E. Tenckhoff, Deformation Mechanisms, Texture, and Anisotropy in zirconium and Zircaloy, (STP 966, Philadelphia, 1988).

[11] A.J.G. Maroto, R. Bordoni, M. Villegas, A.M. Olmedo, M.A. Blesa, A. Iglesias, P. Koenig, J. Nucl. Mater. 229 (1996) 79.

[12] G. Wikmark, P. Rudling, B. Lehtinen, B. Hutchinson, A. Oscarsson, E. Ahlberg, in: Proceedings of 11th International Symposium on Zirconium in the Nuclear Industry, ASTM STP 1295, 1996, p. 55.

[13] J. Godlewski, P. Bouvier, G. Lucazeau, L. Fayette, in: Proceedings of 12th International Symposium on Zirconium in the Nuclear Industry, ASTM STP 1354, 1998, p. 877.

[14] X. Iltis, F. Lefebvre, C. Lemaignan, J. Nucl. Mater. 224 (1995) 109.

[15] M.G. Glavicic, J.A. Szpunar, Y.P. Lin, J. Nucl. Mater. 245 (1997) 147.

[16] R.G. Garvie, P.N. Nicholson, J. Am. Ceram. Soc. 55 (1972) 303.
[17] R. Fillit, P. Homerin, J. Schafer, H. Bruyas, F. Thevenot, J. Mater. Sci. 22 (1987) 3566.
[18] H. Li, Textools Software, Resmat. Corp. (1998–2002).
[19] H. Li, M.G. Glavicic, J.A. Szpunar, Mater. Sci. Eng. A 366 (5) (2004) 164.
[20] N. Petigny, P. Barberis, C. Lemaignan, Ch. Valot, M. Lallemant, J. Nucl. Mater. 280 (2000) 318.
[21] F. Garzarolli, H. Seidel, R. Tricot, J.P. Gros, in: Proceedings of 9th International Symposium on Zirconium in the Nuclear Industry, ASTM-STP 1132, 1991, p. 395.
[22] P. Barberis, J. Nucl. Mater. 226 (1995) 34.
[23] B.D. Cullity, Elements of X-Ray Diffraction, 2nd Ed., Addison-Wesley Publishing Company, 1978.
[24] H. Boysen, F. Frey, Acta Crystallogr. B 47 (1991) 881.
[25] J. Lin, H. Li, J.A. Szpunar, R. Bordoni, A.M. Olmedo, M. Villegas, A.J.G. Maroto, Mater. Sci. Eng. A, in press.